International Journal of GEOMATE, Oct., 2021, Vol.21, Issue 86, pp.167-179
ISSN: 2186-2982 (P), 2186-2990 (O), Japan, DOI: https://doi.org/10.21660/2021.86.j2263
Geotechnique, Construction Materials and Environment

SHEAR BEHAVIOR OF FIBER-REINFORCED CONCRETE BEAMS: AN EXPERIMENTAL STUDY

*Ahid Zuhair Hamoodi[1], Mustafa Shareef Zewair[2], and Mohammed Farhan Ojaimi[3]

[1]Engineering College, Basrah University, Iraq; [2]Engineering College, Basrah University, Iraq; [3]Engineering College, Basrah University, Iraq

*Corresponding Author, Received: 07 July. 2021, Revised: 31 Aug. 2021, Accepted: 03 Oct. 2021

Abstract: Eight steel fiber-reinforced normal strength concrete beams (200 mm wide, 250 mm deep and 1500 mm long) were tested in bending under two concentrated loads, without and with stirrups. The concrete beams were designed to have marked shear behavior. Three types of steel fibers (SFs), straight, hooked and corrugated, were investigated as a possible replacement for standard transverse reinforcement. The fiber volume content, the aspect ratio of fibers, and the existence of stirrups were the major testing parameters in this regard. Four fiber volume proportions (R_f of 0%, 0.5%, 1.0% and 1.5%) and three aspect ratios (l/d of 50, 55 and 60) were utilized. According to the experimental data, the shear behavior of steel fiber-reinforced normal strength concrete beams (SFRCBs) without stirrups was similar, if not superior, to that of normal strength concrete beams (RCBs) with stirrup reinforcement. The SFRCBs displayed extremely thin diagonal cracks and higher shear strengths, especially for fiber fractions of 1% and 1.5%. The experimental results were compared to major universal codes and existing models from the literature. The major codes undervalue the concrete contribution to shear strength while exaggerating the contribution of the stirrups. Furthermore, some of the existing models overestimate the fibers' contribution to the shear strength, while others underestimate it when compared to the present experimental findings.

Keywords: Steel fiber-reinforced concrete, Transverse reinforcement, Steel fiber volume content, Diagonal cracking, Shear strength, Span depth ratio.

1. INTRODUCTION

Structural concrete is extensively utilized in engineering projects. Many factors influence the shear behavior of reinforced concrete beams (RCBs), making them hard to address. Among these factors are the combined effect of shear, axial, bending or torsion loads that many RCBs are subjected to, the quantity and diameter of stirrups, the bond between steel bars and surrounding concrete, aggregate interlock, dowel action, or cement type [1].

Recently, RC with steel fibers (SFs) has been broadly used in civil engineering projects [2]. SFs can enhance the shear strength of RCBs, change the brittle shear behavior to ductile behavior, restrict crack width, spacing and propagation and increase the energy dissipation [3, 4].

When the RCB is subjected to tensile stresses higher than its tensile strength, cracks develop. As in RCBs, the greatest shear stress of steel fiber-reinforced concrete beams (SFRCBs) is related to the effective depth (d), span to depth ratio (a/d) and main steel reinforcement ratio (ρ). The shear strength of RCB can be enhanced by increasing the effective depth (i.e., delaying the initiation of diagonal shear cracks) or increasing the value of a/d, while shear failure can be guaranteed with an adequate quantity of main steel reinforcement. Additionally, the number of fibers per volume, aspect ratio (l/d), and fiber shape control the shear stress in SFRCBs [5]. Previous investigations have been conducted to provide a good database for the shear behavior of SFRCBs.

In 2000, Noghabai [6] experimentally studied the behavior of SFRCBs. The variables were the beam dimensions, shear spans, and types of fibers. According to the results, the inclusion of SFs was necessary, especially for the occurrence of flange tension failure. On the other hand, beams with mixed SFs (different length to diameter ratios and shapes) had better behavior than those with a single fiber type.

Kim et al. 2008 [7] studied the influence of the types and content of fibers on the behavior of high-strength SFRCBs. The findings revealed that the structural behavior of beams with high-strength twisted fibers outperformed that of beams with other fiber types.

Gregori et al. 2016 [1] performed experimental and numerical work to investigate the role of SFs in the shear strength of concrete. Uncracked push-off RC and SFRC specimens were tested. Accurate photogrammetry was used to measure normal and transverse strain close to the shear plane. The experimental tests showed that the shear strength of SFRC specimens is greater than that of RC specimens. On the other hand, the reinforcement passing the shear plane extensively controls the shear enhancement of SFs following diagonal cracking. At the same time, good agreement with the

experimental results was attained by numerically modeling the RC and SFRC push-off specimens. Yoo and Yang 2017 [8] investigated the shear behavior of SF high-strength RCBs (SFHRCBs). This work discussed the influence of transverse reinforcement, SF, and beam size on the shear performance of the beams. The experimental results showed that the shear strength of the SFHRCB without stirrups decreased with increasing beam size. On the other hand, the spread of cracks can be restricted with the presence of SFs. The beams with minimum stirrups exhibited improved shear cracking behavior compared with those reinforced with SFs. In 2018, the shear strength of reinforced concrete, industrial SFRC and recycled SFRC was studied experimentally and theoretically by Leone et al. [9]. The results showed acceptable toughness and shear performance of recycled SFRC relative to industrial SFRC.

2. RESEARCH IMPORTANCE

The importance of steel fiber-reinforced concrete (SFRC) lies in the need to enhance the tensile strength of concrete under large applied loads, vibration loads and impact loads [10]. The shear strength of RCBs is a complicated issue due to the interference of several factors related to loading, beam geometry, and main and transverse reinforcement; therefore, the present work evaluated the role of steel fibers in the improvement of concrete mechanical characteristics and upgrading the shear behavior of RCBs.

3. DESCRIPTION OF MATERIALS AND SPECIMENS

3.1 Geometric Details of the Specimens

Fig. 1 depicts the specifics of the stirrups and the main reinforcement of the tested beams. In this work, a total of 8 RCBs, 200 mm wide, 250 mm deep and 1500 mm long, were strengthened with different volumetric ratios and types of SF. One beam reinforced transversely with vertical stirrups (containing no SFs), as shown in Fig. 1a, was denoted as SS. The other tested beams without stirrups and containing SFs of different R_f and l/d values and types were identified as S1, S2, S3, S4, S5, S6 and S7, as shown in Fig. 1b.

3.2 Reinforcement Bars

Rebars of 8 mm diameter were employed for the stirrups, while 12 mm and 16 mm diameter rebars were used for the top and bottom main reinforcement, respectively. Moreover, the bottom and top of the steel bar areas were 804.25 mm^2 and 226.2 mm^2, respectively, and the bars were arranged in the same way in all the beams. Table 1 depicts the results of the direct tension test of the deformed bars.

3.3 Steel Fibers

Straight, 3 cm hooked, 5 cm hooked and corrugated SFs (Fig. 2) were used in the RCBs. The details of these SFs are presented in Table 2. Straight SFs were included in the concrete mix at four ratios by volume: 0%, 0.5%, 1% and 1.5%. On the other hand, hooked and corrugated SFs were included in the concrete at a ratio of 1% by volume.

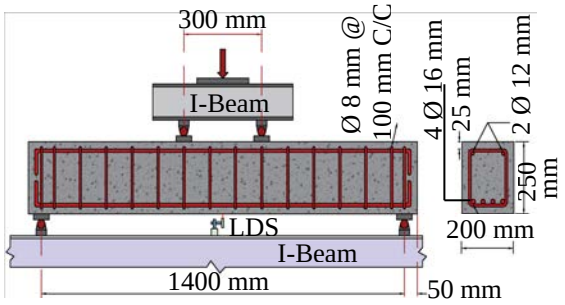

(a)

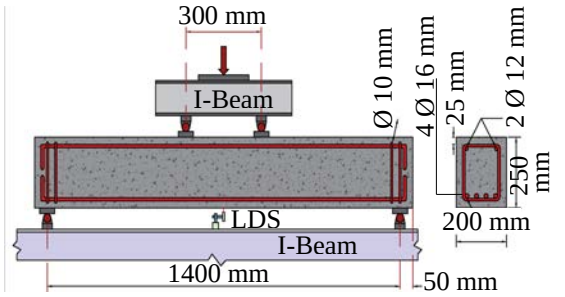

(b)

Fig. 1 Specifics of the beam and the test device

Table 1 Results of the direct tension test

Bar diameter (mm)	8	12	16
fy (MPa)	370	474	525
fu (MPa)	495	564	674
εy (%)	12.76	12.79	12.88
εu (%)	25.31	25.33	25.64
Es (GPa)	209.23	209.28	210.14

Table 2 Details of the steel fibers (by supplier)

Fiber type	Straight	Hooked* (3 cm)	Hooked* (5 cm)	Corrugated
D kg/m^3	7860	7860	7860	7860
f_t MPa	2850	≥ 1000	≥ 1000	≥ 700
L mm	12	30	50	30
d mm	0.25	0.5	0.9	0.55**
l/d	50	60	55	55
E_{SF}	2×10^5	2×10^5	2×10^5	2×10^5

** Hooked ends and straight middle, ** Equivalent diameter, D=density, f_t= tensile strength, L=length, d= diameter, l/d = aspect ratio, E_{SF} = modulus of elasticity of SF.*

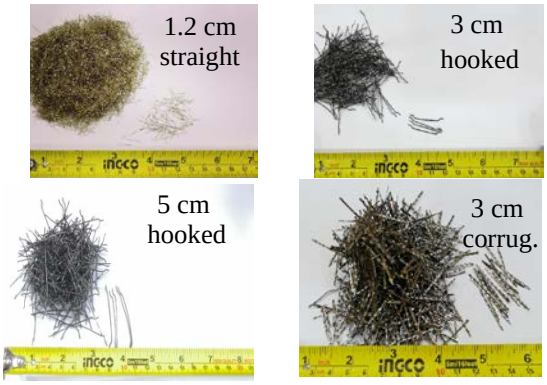

Fig. 2 Types of steel fibers

3.4 Coarse and fine aggregates

Natural sand and (20–5 mm) crushed gravel from the Al-Zubair region, Basrah, Iraq, were used in this study. Based on ASTM C33/C33M-18 [11], both types of aggregates were tested. The fineness modulus of the used sand was 2.78. Table 3 shows the grading of both types of aggregates.

Table 3 The grading of fine and coarse aggregates

Coarse aggregates			Fine aggregates		
Sieve size mm	Passing %	ASTM C33/ C33M-18	Sieve size mm	Passing %	ASTM C33/ C33M-18
25	100	100	9.5	100	100
19	100	90–100	4.75	99	95–100
12.5	80	---	2.36	90	80–100
9.5	37	20–55	1.18	75	50–85
4.75	2	0–10	0.60	53	25–60
2.36	1	0–5	0.30	17	5–30
1.18	0	---	0.15	2	0–10
0.3	0	---	0.075	0	0–3

3.5 Concrete Mix

Cement, sand, gravel, SFs, water and ViscoCrete F-180G superplasticizer were mixed to produce the required concrete composition. In addition, the superplasticizer was added to the solution until the SFs were entirely discrete. The concrete mix details are given in Table 4. It should be noted that the use of SFs caused an important reduction in the workability of concrete since the relative movements of all concrete components were hindered by SFs. The same effect was observed in previous studies [4].

A constant water/cement (w/c) ratio of 0.49 was employed. For each SF volume ratio, three concrete cubes (150×150×150 mm), three concrete cylinders (150×300 mm) and three concrete prisms (100×100 × 350 mm) were cast and tested in a hydraulic testing machine to evaluate the concrete strength. Based on BS EN 12390:1-3 [12], ASTM C496/C496M-17 [13] and ASTM C78/C78M [14], the compressive strength, tensile strength and modulus of rupture of concrete were found, respectively, as presented in Table 5.

3.6 Loading and test setup of beams

Eight simply supported beams were produced with a constant a/d of 2.657 to study the shear behavior. A four-point bending test was performed by two concentrated line loads 300 mm apart and two round bars to support the 1500 mm span beams, as shown in Fig. 3. The test was conducted using a 2000 kN hydraulic Torsee universal testing machine under displacement control conditions. The failure of the beam was the end of the test. The midspan deflection was recorded at every loading stage using a laser displacement sensor, as shown in Figs. 1 and 3. Additionally, the crack width was gauged by adopting an HFBTE CK-102 digital concrete crack width gauge tester meter, as presented in Fig. 3.

4. EXPERIMENTAL RESULTS

4.1. Strength of Fiber-Reinforced Concrete

4.1.1 Compressive strength

The 28-day average cube compressive strengths corresponding to different straight SF amounts are presented in Table 5. Fig. 4 shows the effect of the straight SF volume content on various relative strengths of concrete. The compressive strength was enhanced by approximately 32.30% when straight SFs up to 1.5% by volume were used in the concrete.

4.1.2 Flexural strength

The flexural strength of fiber-reinforced concrete was measured by calculating the modulus of rupture. Table 5 and Fig. 4 show the 28-day average modulus of rupture for various straight SF contents. The increase in the content of straight SFs from 0% to 1.5% by volume caused a great increase in flexural strength of approximately 82.6%, with remarkable ductile failure.

4.1.3 Splitting tensile strength

Table 5 and Fig. 4 depict a 90.8% increase in splitting tensile strength when a 1.5% straight SF volume content was introduced. This is the largest increase in contrast to compressive and flexural strength, so the inclusion of SFs considerably improves the tensile characteristics and crack resistance of concrete. This finding is consistent with the results obtained in the literature [2, 4, 15].

4.2 Cracking Behavior and Nature of the Failure

When the beams are loaded, flexural cracks are

Table 4 Concrete mix details

Gravel (kg/m^3)	Sand (kg/m^3)	Cement (kg/m^3)	Water (kg/m^3)	Superplasticizer (kg/m^3)	SF (kg/m^3)			
					0%	0.5%	1.0%	1.5%
1110	740	370	181.3	2.22	0.0	12	24	36

Table 5 Beam details and concrete strength test results

Beam details							Concrete strength test results		
Notation	a/d	Shape of SF	*l/d*	ρ (%)	ρ_s (%)	R_f (%)	$f_{cu,ave.}$ (MPa)	$f_{t,ave.}$ (MPa)	$f_{r,ave.}$ (MPa)
SS	2.657	------	------	1.942	0.50	0	35.6	2.29	4.19
S1	2.657	------	------	1.942	0.0	0	35.6	2.29	4.19
S2	2.657	Straight	50	1.942	0.0	0.5	39.3	2.85	5.49
S3	2.657	Straight	50	1.942	0.0	1.0	44.8	3.75	7.0
S4	2.657	Straight	50	1.942	0.0	1.5	47.1	4.37	7.65
S5	2.657	3 cm Hooked	60	1.942	0.0	1.0	43.1	4.57	8.20
S6	2.657	5 cm Hooked	55	1.942	0.0	1.0	43.5	4.30	8.14
S7	2.657	Corrugated	55	1.942	0.0	1.0	44.0	4.16	7.78

ρ = main reinforcement ratio, ρ_s = transverse reinforcement ratio, R_f = steel fiber volume fraction, $f_{cu,ave.}$ = 28-day average cube compressive strength, $f_{t,ave.}$ = 28-day average splitting tensile strength, $f_{r,ave.}$ = 28-day average modulus of rupture.

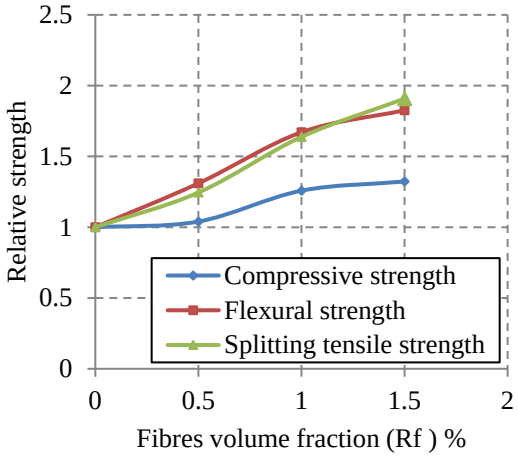

Fig. 4 Influence of the volume content of straight SFs on different relative strengths of concrete

the first to appear vertically in the tension zone at the region of the maximum bending moment. With additional loading (42% to 64% of F_u), diagonal cracks develop in the shear span along the direction of the support and the loading point. In comparison to those in beams without SFs or with an inadequate SF content, diagonal cracks developed at comparatively greater loads than those when an adequate amount of SFs was present (Table 6), and as the load increased, the cracks were efficiently restricted and remained narrower. Fig. 5 shows that the diagonal crack pierced into the compression zone at the loading point, crushing the concrete there, and depicts the effective bridging of the diagonal crack by the SFs spanning it.

For beams without SFs, brittle shear failure occurred by diagonal splitting at a relatively lower load, as in the S1 beam of Fig. 6(b). Ductile shear failure occurred at relatively higher loads with the introduction of straight SFs as in beams S2, S3, and S4 of Fig. 6(c), Fig. 6(d) and Fig. 6(e) respectively, hooked SFs as in beams S5 and S6 of Fig. 6(f), and corrugated SFs as in beam S7 of Fig. 6(g).

SFs successfully minimize crack opening by absorbing tensile stress after cracking [2]. The bent forms of fibers (especially the hooked type), which appear straightened in Fig. 7, demonstrate their effectiveness after cracking. Table 6 shows that the volume fraction of fibers has no direct relationship with the improvement in shear contribution. The load capacity increased by 34% when a straight SF volume fraction of 0.5% was used; however, it was only enhanced by approximately 29% when the straight SF volume content was multiplied by 3, increasing from 0.5% to 1.5%. On the other hand, the use of a 3 cm hooked SF volume fraction of 1% showed an improvement of 21.4% in load capacity compared to that with the straight SFs. This finding is consistent with the results that appeared in the literature [2,16,17]. Table 6 shows the experimental findings for diagonal cracking and ultimate loads for all beams tested. The replacement of the transverse reinforcement with a straight SF volume content of 0.5% has a reverse effect on the ultimate loads, as illustrated in Table 6. On the other hand, the ultimate load may even rise when enough and effective SFs are employed. The usage of 1.0% and 1.5% straight SFs resulted in ultimate load increases of approximately 2.0% and 4.0%, respectively. Similarly, the employment of 1.0% 3 cm and 5 cm hooked SFs and corrugated SFs increased the ultimate loads by approximately 8.0%, 5.0% and 3.0%, respectively. Additionally, compared to beams without stirrups or with inadequate SFs, adequate and effective SFs postpone the growth of diagonal cracking in the same way as stirrups. In this regard, 1.0% SFs appears to be the minimum for enhancing the behavior of conventional concrete in shear. As a result, substituting sufficient SFs for transverse steel appears to enhance both diagonal cracking and ultimate loads.

Table 6 Experimental loads and mode of failure of all tested beams

Beam symbol	a/d	ρ (%)	ρ_s (%)	R_f (%)	*l/d*	F_d (kN)	F_u (kN)	Difference F_u (%) S/SS	Difference F_u (%) S/S1	Failure Mode
SS	2.657	1.942	0.5	0.0	----	146.52	243.26	-----	-----	F-S
S1			0.0	0.0	----	94.50	175	-----	-----	S
S2			0.0	0.5	50	98.23	235	-3.39	+34.29	S
S3			0.0	1.0	50	152.71	247.5	+1.74	+41.43	S
S4			0.0	1.5	50	157.81	252.5	+3.79	+44.29	S
S5			0.0	1.0	60	169.37	263	+8.11	+50.3	F-S
S6			0.0	1.0	55	163.46	255	+4.83	+45.71	S
S7			0.0	1.0	55	153.88	250	+2.77	+42.86	S

F_d = diagonal cracking load, F_u = ultimate load, F-S = flexural-shear, S= shear

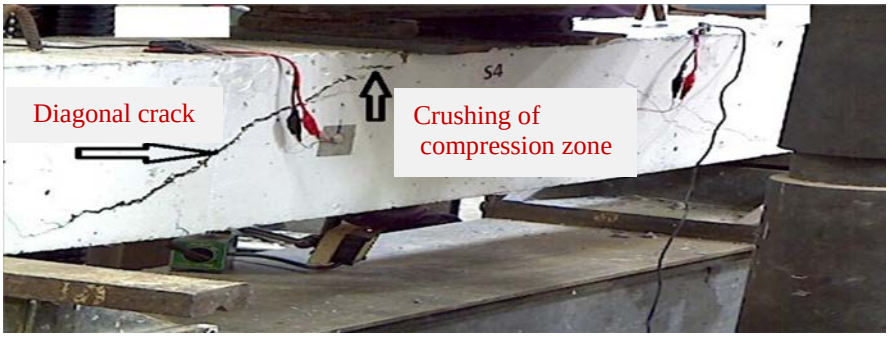

Fig. 5 Diagonal crack in an SF-reinforced concrete beam

(a) Beam SS (with stirrups and without SFs)

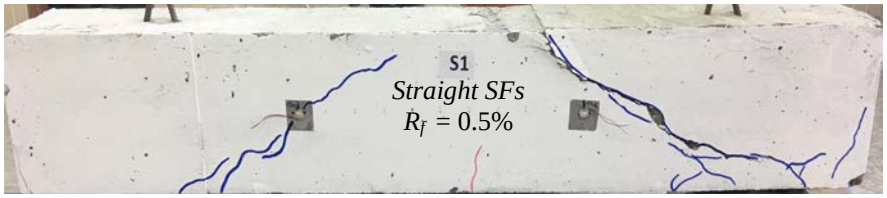

(b) Beam S1 (without stirrups and without SFs)

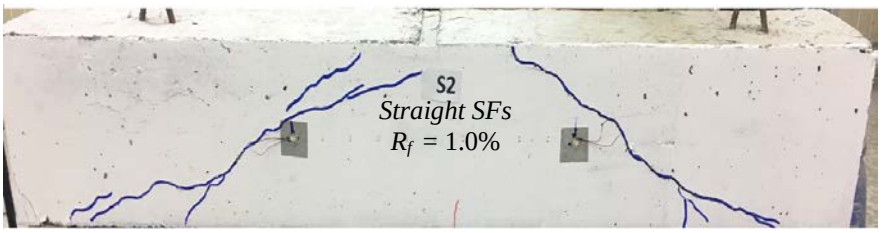

(c) Beams S2 (with 0.5% straight SFs)

Fig. 6 Failure of the tested beams

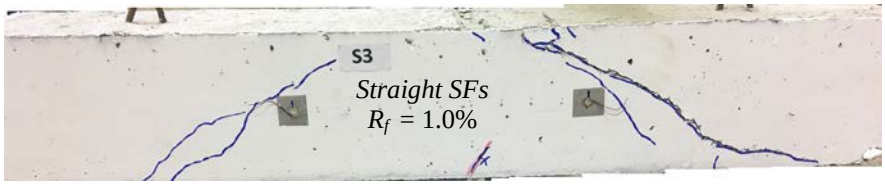

(d) Beams S3 (with 1.0% straight SFs)

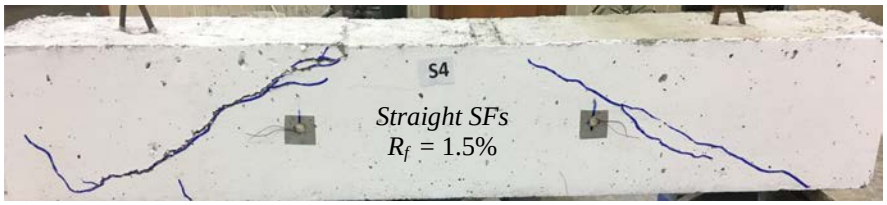

(e) Beams S4 (with 1.5% straight SFs)

(f) Beams S5 and S6 (with 1.0% 3 cm and 5 cm hooked SFs, respectively)

(g) Beam S7 (with 1.0% corrugated SFs)

Fig. 6 Continued

S5, R_f =1.0% S6, R_f =1.0% S7, R_f =1.0%

Fig. 7 Deformation of fibers after failure

4.3 Load-Deflection Characteristics

Fig. 7 illustrates the load-deflection curves of the tested beams. From the initial loading to the formation of the first crack, all of the beams displayed linear behavior. After cracks formed, all of the beams showed nonlinear behavior. At this stage, the deflection rises in tandem with load but at a faster rate. The beam without transverse reinforcement and SFs (S1) lost its stiffness and failed without undergoing further significant deformation after complete cracking and growth of the cracks, in comparison to those with stirrups (SS) or with SF reinforcement. Therefore, SFs serve the same purpose in restraining cracks as stirrups and consequently maintain a considerably higher stiffness that is less impacted by the smaller cracks. The final stage refers to the concrete beam's plastic flow or behavior, which causes significant plastic deflections prior to failure. Lim and Oh [15], Tahenni, Chemrouk and Lecompte [16], Narayanan and Darwish [18], and Furlan and Hanai [19] all obtained the same results.

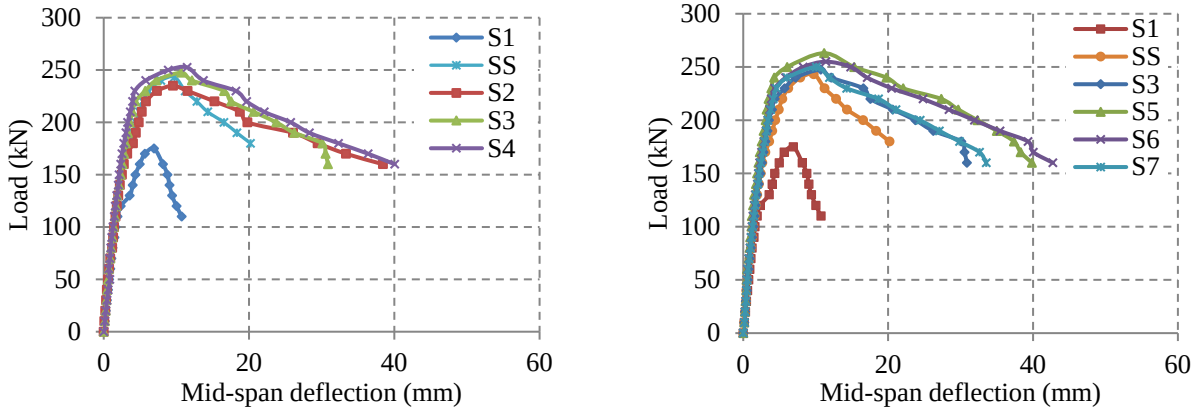

(a) (b)

Fig. 7 Load-deflection relationships: (a) effect of straight SF volume content, (b) effect of SF types

4.4 Ductility

The displacement ductility ratio (DR) suggested by Cohn and Bartlett [20, 21] was used to determine the ductility of SFRC beams. According to this method, the ductility index (DR) is the ratio of the displacement at 85% of the ultimate load ($\Delta_{0.85}$) to the first yield displacement of the specimen (Fig. 8): $DR = \Delta_{0.85} / \Delta_y$.

Fig. 9 below depicts the ductility index of all tested beams. The ductility of the SFRCB rises as the volume fraction and aspect ratio of fibers increase, as seen in Fig. 9. This result demonstrates that replacing transverse reinforcement with SFs at an optimal dose ($R_f \geq 1.0\%$) improves the ductility of RC beams.

4.5 Diagonal Crack Widths

The crack widths at the diagonal cracking load and ultimate load are shown in Fig. 10. This figure indicates that the cracks were well restricted when SFs were utilized, and their width did not exceed the serviceability limit of 0.3 mm until immediately before failure. The cracks in SF-reinforced beams remained very narrow in comparison to cracks in beams without SFs (S1). As indicated in Table 6, the SFs helped to delay the emergence of diagonal cracks. This behavior is consistent with the results obtained in the literature [2, 15, 16, 22, 23].

A vision-based technique for damage progress monitoring of the structure under the loading regime was used. As shown in Fig. 11, successive images for a diagonal crack at constant travel time were captured using a camera and stored automatically on a PC for posttest analysis. SFs appear to be extremely effective in enhancing the serviceability of concrete in real-world constructions. Because cracking that is too wide is responsible for several problems that require retrofitting and repair in the building sector and may even cause failure if not properly cared for, serviceability will be an important design requirement [16].

4.6 Analysis of Shear Strength of Concrete Beams

It is widely accepted that in an RC beam, the ultimate shear force V_u is resisted by the uncracked portion of the concrete V_{cz}, across the interlocking of the surface roughnesses V_{iy}, across the longitudinal steel V_d acting as a dowel, and by the influence of stirrups V_s [24], as shown in Fig. 12 below. The ultimate shear force can be expressed as:

$$V_u = V_{cz} + V_{iy} + V_d + V_s \quad (1)$$

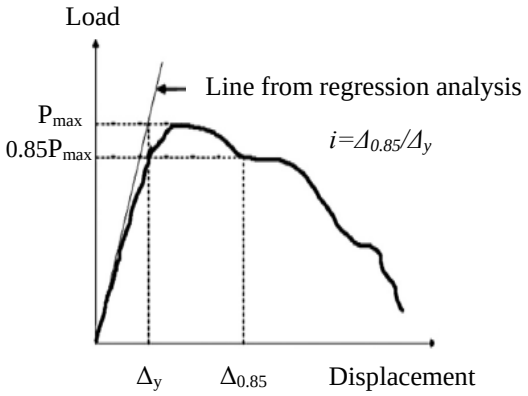

Fig. 8 Displacement ductility index according to Cohn and Bartlett [19, 20]

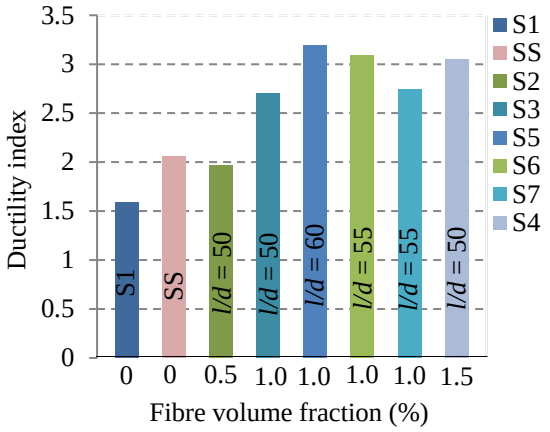

Fig. 9 Ductility ratio of the tested beams

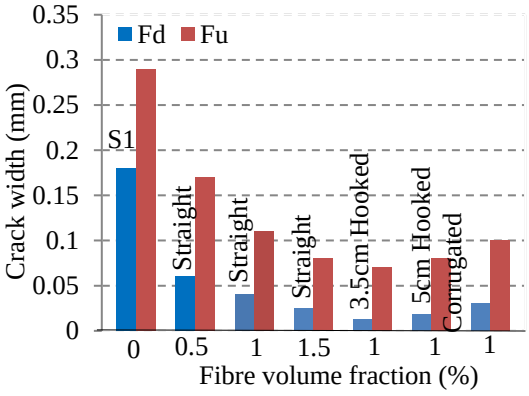

Fig. 10 Crack widths at diagonal cracking and ultimate loads

The concrete contribution to shear resistance V_c is defined as $(V_{cz} + V_{iy} + V_d)$. It has been described [25, 26] that $V_{cz} = 20 - 40\%$ of V_u, $V_{iy} = 35 - 50\%$ of V_u, and $V_{iy} = 15 - 25\%$ of V_u are the three components of the involvement of concrete in shear resistance. It should be noted that these three components and their interactions have yet to be fully characterized, and no analytical approach for rationally combining these parameters exists. The

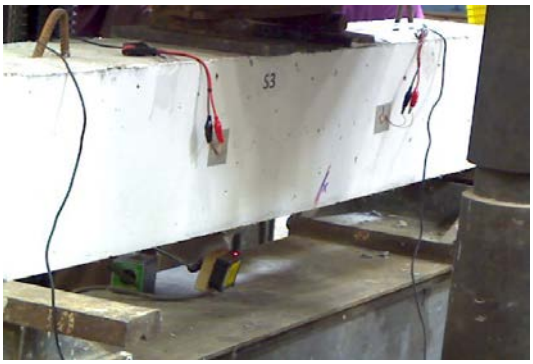

At 25% of ultimate load (no diagonal cracking)

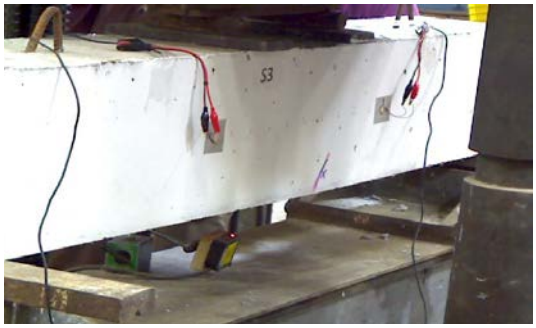

At 50% of ultimate load

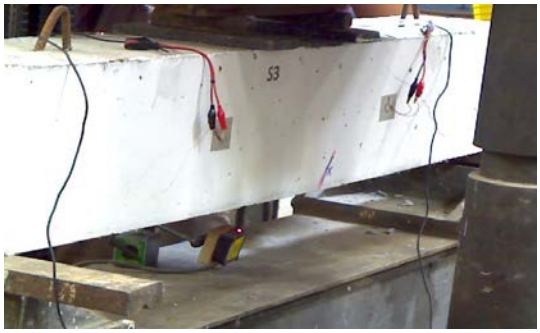

At 65% of ultimate load (diagonal cracking at right support)

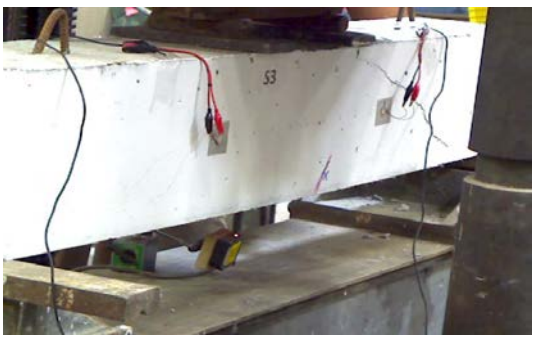

Just before failure

Fig. 11 Development of diagonal cracking in an SFRCB

application of various empirical formulas in design around the world warrants the topic's ongoing investigation [16].

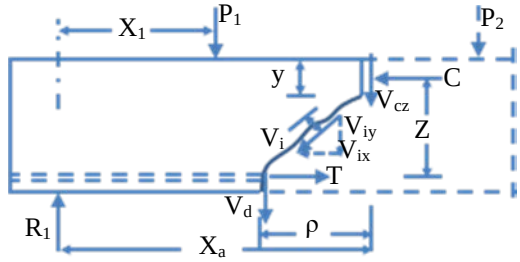

Fig. 12 Shear forces in an RC beam with web reinforcement [24]

4.6.1 Theoretic prediction of the shear strength

Table 7 summarizes the main methods for determining the V_u of RC beams as specified in various design codes, namely, ACI318-19, BS8110 and EC2. These theoretical shear estimations are for maximum compressive strengths of 60 MPa in concrete.

Where stirrups are included, the shear strength of RCB is the sum of V_c and V_s, as given by Eq. (1) above. Because the S1 beam is not strengthened transversally, its ultimate shear strength is calculated by the concrete V_c. The value of the ultimate shear strength of the S1 beam is presented in Table 8 and Fig. 13. The suggested universal codes also forecast the ultimate shear strength of the S1 beam. The findings reveal that all models of the codes undervalue the shear contribution of conventional concrete. EC2 is the most accurate of the three models, although it still underestimates the shear capacity of concrete by approximately 45%. On the other hand, V_u is considerably underestimated by 55% below the test value when the ACI code iss applied.

Table 8 and Fig. 13 demonstrate the involvement of V_s in the shear strength of the SS beam. V_c accounts for 72% of the total shear capacity, whereas V_s accounts for 28%. Hereafter, the addition of stirrups increased the ultimate shear strength of the normal RCB by approximately 30%. The shear strength influence of the stirrups of the SS beam is calculated by the three main codes is and shown in Table 8 and Fig. 13 for comparison. It is obvious that these codes considerably overestimate the contribution of transverse reinforcement to the shear strength of normal RCB. The reason is that the equations of the three models are built on the yielding of this reinforcement, as indicated by the formulations of codes in Table 7. These models do not account for concrete crushing in the inclined strut or at the compression zone immediately at the end of a diagonal crack. Therefore, for beams with smaller a/d values, any shear design method built on the yielding of the stirrups may not be safe, as failure will happen before the yielding of the stirrups [16].

Eurocode 2 appears to give the best expectations for V_u of the three code models when the shear resistance of normal concrete beams includes the concrete and steel contributions, although it is still impractical due to undervaluing the concrete contribution V_c and highly overestimating the transverse reinforcement contribution V_s.

4.6.2 Influence of steel fibers on the shear strength

Straight SFs enhanced the shear and ultimate load capacities of normal concrete beams, with increases ranging from 34% for an R_f of 0.5% to 44% for an R_f of 1.5%. For an R_f of 1%, this increase was 50.3%, 45.7%, and 42.86% when 3 cm hooked, 5 cm hooked and corrugated steel fibers were used, respectively.

Various investigations and analytical models have been proposed regarding the influence of SFs on the shear resistance of RCBs [15, 17, 18, 23]. Cucchiara et al. [29] calculated the total ultimate shear force in SFRCBs by summing V_c, V_s, and V_f, as in Eq. (2) below.

$$V_u = V_c + V_s + V_f \quad (2)$$

For SFRCBs without stirrups, such as beams S2, S3, S4, S5, S6 and S7 in this work, the ultimate shear force is presented in Eq. (3), and the components of the shear resistance through the diagonal crack are presented in Fig. 14 below.

$$V_u = V_c + V_f \quad (3)$$

Therefore,

$$V_f = V_u + V_c \quad (4)$$

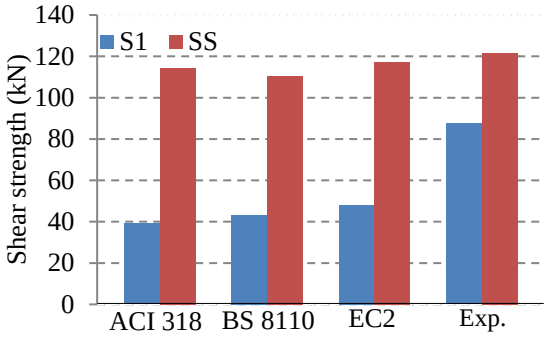

Fig. 13 Experimental and predicted ultimate shear strengths

In Eq. (4), the ultimate shear force V_u is the experimental value $V_{u\,exp.}$, and the involvement of concrete V_c is the shear strength of the S1 beam

Table 7 Ultimate shear strength based on the main worldwide codes

Codes	Equation	Definition
ACI 318-19 [27]	$V_u = V_c + V_s$ $V_c = \left[0.17\,\lambda\sqrt{f_c'} + \frac{N_u}{6\,A_g}\right] b_w d$ or $\left[0.17\,\lambda\,(\rho_w)^{1/3}\sqrt{f_c'} + \frac{N_u}{6\,A_g}\right] b_w d$ $for\ A_v \geq A_{v,min}$ $V_c = \left[0.66\ \lambda_s\,\lambda\,(\rho_w)^{1/3}\sqrt{f_c'} + \frac{N_u}{6\,A_g}\right] b_w d$ $for\ A_v < A_{v,min}$ $V_s = \frac{A_v\,.\,f_{yt}\,.\,d}{S}$ $for\ vertical\ stirrups$ $V_s = \frac{A_v\,.\,f_{yt}\,.\,(\sin\alpha + \sin\alpha).\ d}{S}$ $for\ inclined\ stirrups$	f_c'= cylinder compressive strength N_u = axial load A_g= gross area of concrete section b_w = width of beam d= effective depth λ= 1.0 for normal concrete ρ_w= ratio of A_s to b_w.d λ_s= size effect modification factor $= \sqrt{\frac{2}{(1+0.004d)}} \leq 1.0$ A_v= area of shear reinforcement within spacing *s* $A_{v,min}$= minimum area of shear reinforcement within spacing *s* S= center-to-center spacing of stirrups α = angle between the inclined stirrups and the longitudinal axis of the member f_{yt} = yield strength of transverse reinforcement f_{sv} = yield strength of stirrups $\rho = A_s / b_w d$ f_{cu} = compressive strength of a cube γ_m = 1.25, partial shear safety factor of material α = inclination of stirrups (α = 90°) θ = 45°, the angle between inclined concrete struts and the main tension chord $k = 1 + \sqrt{\frac{200}{d}}, d\ (mm)$ z = lever arm = 0.9d
BS 8110 [28]	$V_u = \frac{0.79}{\gamma_m}\,(100\rho)^{\frac{1}{3}}\,\left(\frac{400}{d}\right)^{\frac{1}{4}}\left(\frac{f_{cu}}{25}\right)^{\frac{1}{3}} b_w\,d + 0.875\,\frac{A_v\,f_{sv}\,d}{S}$ for $^{a}/_{d} \geq 2$ $V_u = \left(2\,\frac{d}{a}\right)\frac{0.79}{\gamma_m}\,(100\rho)^{\frac{1}{3}}\,\left(\frac{400}{d}\right)^{\frac{1}{4}}\left(\frac{f_{cu}}{25}\right)^{\frac{1}{3}} b_w\,d + 0.875\,\frac{A_v\,f_{sv}\,d}{S}$ for $^{a}/_{d} < 2$	
EC2 [29]	$V_u = 0.18\left[k\,.\,(100\,.\,\rho\,.\,f_c)^{\frac{1}{3}}\right] b_w\,d + \frac{A_v\,f_{sv}\,z\,(\cot\theta + \cot\alpha)}{S}\ \sin\alpha$	

Table 8 Experimental and predicted shear strengths

Beam No.	$V_{u,\,exp.}$ (kN)	$V_{s,\,exp.}$ (kN)	$V_{u,\,theo}$ (kN)			$V_{s,\,theo.}$ (kN)			$V_{u,exp.}$ / $V_{u,\,theo}$		
			ACI 318	BS 8110	EC2	ACI 318	BS 8110	EC2	ACI 318	BS 8110	EC2
S1	87.5	----	39.20	43.31	48.13	------	------	------	2.23	2.02	1.82
SS	121.63	34.13	114.56	110.68	117.39	77	67.37	69.26	1.06	1.09	1.04

(without stirrups and SFs) in the present study. If there are no test results, V_c can be estimated using the theoretical models of various codes that were previously provided.

Eq. (4) can be expressed in terms of stresses by dividing both sides by the effective concrete section bd as:

$$v_f = v_u + v_c \quad (5)$$

Eq. (5) depicts the experimental shear strength conveyed by fibers (v_f). The present results revealed out that the shear strength contribution of fibers is dependent on the quantity of fibers utilized R_f and their aspect ratio *l*/*d*. Therefore, the longer the fiber is, the better it is at bridging the two sides of a crack. At a specified fiber content, the smaller the diameter of a fiber is, the greater the number of fibers, and the more bridging activities occurring through a crack, causing a greater fiber involvement in the shear capacity. These effects are in line with the findings of earlier studies [2, 15, 16]. Furthermore, the bond between SFs and concrete is critical in preventing fibers from slipping and pulling of the concrete across a crack. The steel fiber appears anchored on both sides of the crack when it develops; therefore, any influence of these fibers on shear capacity is highly reliant on the fineness of this anchorage and hereafter on the anchoring bond capacity [16].

Prevailing models available in the literature (Table 9) to calculate the influence of the fibers on the shear capacity were investigated for comparison. Table 10 lists the projected values, which are depicted in Fig. 15 with the current test findings. The findings of the current study depict that the contribution of SFs to shear strength increases with increasing R_f and *l*/*d* values of the fibers. Increasing the volume content of straight SFs from 0.5% to 1.5% increases this contribution from 0.73 MPa to 0.94 MPa, respectively, while for 3 cm hooked SFs (l/d = 60, R_f = 1.0%), the involvement of SFs in the shear capacity is 1.07 MPa. Table 10 and Fig. 15 clearly show that the involvement of fibers in the shear capacity is overestimated in some of the existing models, as seen in Fig. 15, and should be considered with caution since they may lead to

insecure design. Additionally, the model suggested by Tahenni, Chemrou and Lecompte [16] and the model suggested by Swamy, Jones and Chiam [23] appear to give the best prospects for v_f of the five models, and they underestimate the SF contribution v_f to shear strength.

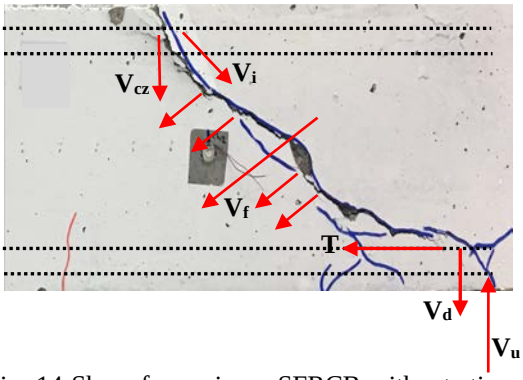

Fig. 14 Shear forces in an SFRCB without stirrups

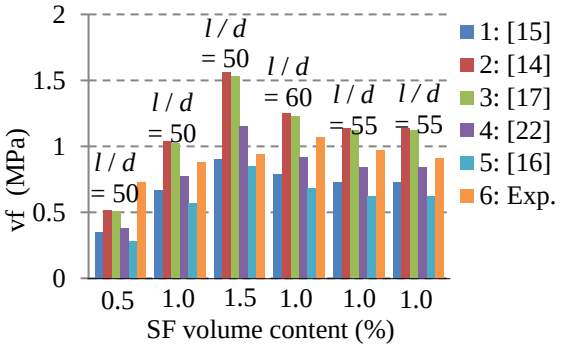

Fig. 15 Experimental and theoretical shear strength of fibers

Table 9 Available models for the involvement of the fibers in the shear capacity

Research	Model	Definitions
Tahenni et al. [16]	$v_f = 0.28\sqrt{f_c}(1-20\rho_f)\rho_f \, {l_f}/{d_f}$	ρ_f = fiber volume fraction l_f/d_f = aspect ratio of fibers
Lim and Oh [15]	$v_f = 0.5\tau V_f \frac{l_f}{d_f} ctg\alpha$	τ = the average fiber–matrix bond stress assumed by [10 in 2] as 4.15 MPa
Narayana and Darwish [18]	$v_f = 0.41\tau k V_f \frac{l_f}{d_f}$	α = 45°, the inclination between the longitudinal reinforcement and the shear crack
Swamy et al. [23]	$v_f = 0.37\tau V_f \frac{l_f}{d_f}$	
Al-ta'an and Al-Feel [17]	$v_f = \frac{8.5}{99} k V_f \frac{l_f}{d_f}$	k = 1.2, the bond factor that accounts for differing

Table 10 Comparison of the experimental results with the available models

Beam No.	R_f (%)	l/d	$v_{u\,exp.}$ (MPa)	$v_{f\,exp.}$ (MPa)	$v_{f\,theoretical}$ (MPa)				
					[15]	[14]	[17]	[22]	[16]
S2	0.5	50	2.84	0.73	0.35	0.52	0.51	0.38	0.28
S3	1.0	50	2.99	0.88	0.67	1.04	1.02	0.77	0.57
S4	1.5	50	3.05	0.94	0.90	1.56	1.53	1.15	0.85
S5	1.0	60	3.18	1.07	0.79	1.25	1.23	0.92	0.68
S6	1.0	55	3.08	0.97	0.73	1.14	1.12	0.84	0.62
S7	1.0	55	3.02	0.91	0.73	1.14	1.12	0.84	0.62

5. Conclusions

The following conclusions can be drawn from the current experimental study on the influence of fibers on the behavior of normal strength concrete, mainly on shear:

- Steel fibers improve the compressive strength, splitting tensile strength and flexural strength.

The gain in strength is highest in splitting tensile strength. Steel fibers can considerably improve the tensile strength and concrete characteristics and increase the resistance to fracturing.

- The SFs effectively restrict cracks and absorb residual forces beyond cracking. Furthermore, SFs spanning diagonal fissures effectively bridge them. Crack creation is delayed, and their width is tightly controlled; even at failure, they did not exceed the serviceability limit of 0.3 mm. In the presence of efficient fibers (with higher l/d values), the failure of the beams transitioned from shear to flexure-shear. By modifying the failure mode, SFs increased the ultimate load capacity of the RCBs.

- The inclusion of SFs significantly improves the ductility of normal strength concrete beams. When sufficient and effective SFs were employed, ductility indices as high as 3.19 were attained. This ductile behavior is very important in seismic areas to prevent brittle and disastrous failures, as seen in numerous earthquake-prone areas across the world [31,32].

- The concrete involvement in the shear capacity of normal strength concrete beams is undervalued by the main worldwide codes, whereas the transverse steel contribution is overvalued. The analogy used to estimate the transverse steel contribution is built on the yielding of stirrups and does not include the crushing failure of concrete before such yielding at the critical shear regions, as is common in beams with smaller a/d values. The current study demonstrated that sufficient steel fibers could definitely replace such transverse reinforcement.

- The inclusion of straight SFs increases the shear strength by 35% for a quantity of fibers R_f of 0.5% to 44.5% for an R_f value of 1.5%, exceeding the upgrading observed with transverse reinforcement when higher amounts of fibers are utilized. Furthermore, the inclusion of effective SFs at a 1% volume content increases the shear strength by 50.7% for 3 cm hooked SFs, 46% for 5 cm hooked SFs and 43% for corrugated SFs. However, the rate of increase is not proportional to the amount of fiber used. The fibers' aspect ratio and the quality of their bond with the cement paste appear to be major factors in the contribution of fibers to shear strength.

6. References

[1] Juan N. G., Eduardo J. M. A., Pedro S. R., and Javier E. O., Experimental Study on The Steel-Fibre Contribution to Concrete Shear Behaviour, Construction and Building Materials, Vol. 112, 2016, pp. 100-111.

[2] Meda A., Minelli F., Plizzari G. A., and Riva P., Shear Behaviour of Steel Fibre Reinforced Concrete Beams, Material and Structures, Vol. 38, 2005, pp. 343-351.

[3] Yining D., Zhiguo Y., and Said J., The Composite Effect of Steel Fibres and Stirrups on The Shear Behaviour of Beams Using Self-Consolidating Concrete, Engineering Structures, Vol. 33, 2011, pp. 107–117.

[4] Hamid R. C., Mansour G., Arash K., Jorge de B., and Mohsen K., Shear Behaviour of Concrete Beams With Recycled Aggregate and Steel Fibres, Construction and Building Materials, Vol. 204, 2019, pp. 809–827.

[5] Masoud A., Ali K., Ahmad D., Mahdi K., New Empirical Approach for Determining Nominal Shear Capacity of Steel Fiber Reinforced Concrete Beams, Construction and Building Materials, Vol. 234, 2020, pp. 117293.

[6] Nogababi K., Beams of Fibrous Concrete in Shear and Bending, Journal of Structural Engineering, Vol. 126, 2000, pp. 243-251.

[7] Kim D. J., Naaman A. E., and El-Tawil S., Comparative Flexural Behaviour of Four Fibre Reinforced Cementitious Composites, Cement and Concrete Composites, Vol. 30, 2008, pp. 917–928.

[8] Doo Y. Y., and Jun M. Y., Effects of Stirrup, Steel fiber, and Beam Size on Shear Behavior of High-Strength Concrete Beams, Cement and Concrete Composites, 2018, doi: 10.1016/j.cemconcomp.2017.12.010.

[9] Leone M., Centonze G., Colonna D., Micelli F., and Aiello M.A., Fiber-Reinforced Concrete With Low Content of Recycled Steel Fiber: Shear behaviour, Construction and Building Materials, Vol. 161, 2018, pp. 141–155.

[10] Zewair M. S., Hamoodi A. Z., and Ojaimi M. F., Effect of Types of Fibres on the Shear Behaviour of Deep Beam with opening, Periodicals of Engineering and Natural Sciences, Vol. 9, No. 2, 2021, pp. 1086-1095.

[11] ASTM Standard C33/C33M – 18, Standard Specification for Concrete Aggregate, ASTM International, West Conshohocken, PA 19428-2959, United States, 2019.

[12] BSEN 12390-3, Method for Determination of Compressive Strength of Concrete Cubes, published by BSI, 2009.

[13] ASTM Standard C496/C496M – 17, Standard Test Method for Splitting Tensile Strength of Cylindrical Concrete Specimens, ASTM International, West Conshohocken, PA 19428-2959, United States, 2018.

[14] ASTM Standard C78/C78 – 18, Standard Test Method for Flexural Strength of Concrete (Using Simple Beam with Third-Point Loading), ASTM International, West Conshohocken, PA 19428-2959, United States, 2019.

[15] Lim D. H., Oh B. H., Experimental and Theoretical Investigation on The Shear of Steel Fiber Reinforced Concrete Beams, Eng. Struct., Vol. 21, 1999, pp. 37–44.

[16] Tahenni T., Chemrouk M., and Lecompte T., Effect of Steel Fibers on The Shear Behavior of High Strength Concrete Beams, Construction and Building Materials, Vol. 105, 2016, pp. 14–28.

[17] Al-Ta'an S. A., and Al-Feel J. R., Evaluation of Shear Strength of Fiber Reinforced Concrete Beams", Cement and Concrete Composites, Vol. 12, Issue 2, 1990, pp. 87–94.

[18] Narayanan R., and Darwish I. Y. S., Use of Steel Fibers as Shear Reinforcement, ACI Struct. J., Vol. 84, Issue 3, 1987, pp. 216–227.

[19] Furlan S. Jr., and de Hanai J. B., Shear Behaviour of Fiber Reinforced Concrete Beams, Cement and Concrete Composites, Vol. 19, 1997, pp. 359–366.

[20] Mansour G., Arash K., and Jorge de B., Influence of Steel Fibres on The Flexural Performance of Reinforced Concrete Beams With Lap-Spliced Bars", Construction and Building Materials, Vol. 229, 2019, pp. 116853.

[21] Cohn M. Z., and Bartlett M., Computer-Simulated Flexural Test of The Partially

Prestressed Concrete Section, ASCE J. Struct. Div., Vol. 5, 1982, pp. 2747–2765.
[22] Li V. C., and Leun G. C. K. Y., Steady-State and Multiple Cracking of Short Random Fiber Composites, J. Eng. Mech.-ASCE, Vol. 118, Issue 11, 1992, pp. 2246–2264.
[23] Swamy R. N., Jones R., and Chiam A. T. P., Influence of Steel Fibers on The Shear Resistance of Lightweight Concrete T-Beams, ACI Struct. J., Vol. 90, Issue 1, 1993, pp. 103–114.
[24] Arthur H. N., David D., Charles W. D., Design of Concrete Structures, Fourteenth Edition in SI Units, McMraw-Hill Companies Inc., 2010, pp. 1-742.
[25] Taylor H. P. J., The Shear Strength of Large beams, Proc. ASCE, Vol. 98, 1972, pp. 2473–2490.
[26] Fenwick R. C., Paulay T., Mechanisms of Shear Resistance of Concrete Beams, J. Struct. Div.-ASCE, Vol. 94, 1968, pp. 2325–2350.
[27] ACI Committee 318, Building Code Requirements for Structural Concrete, ACI 318-19, Farmington Hills, Mich, 2019.
[28] BS 8110, Structural Use of Concrete-Part1, Code of Practice for Design and Construction, British Standards Institution, London, 1997, p. 173.
[29] Eurocode 2, Design of Concrete Structures-Part 1–1: General Rules and Rules for Buildings, EN1992-1-1, R, 2004, p. 100.
[30] Cuchiara C., Mendola L., and Papia M., Effectiveness of Stirrups and Steel Fibers as Shear Reinforcement, Cement and Concrete Composites, Vol. 26, Issue 7, 2004, pp. 777–786.
[31] Ashour SA., Effect of Compressive Strength and Tensile Reinforcement Ratio on Flexural Behavior of High-Strength Concrete Beams, Eng Struct., Vol. 22, 2000, pp. 413–23.
[32] Gunasekaran K., Annadurai R., Kumar PS., Study on Reinforced Lightweight Coconut Shell Concrete Beam Behavior Under Flexure, Mater. Des., Vol. 46, 2013, pp. 157–67.